SSRG International Journal of Applied Physics
ISSN: 2350-0301/ https://doi.org/10.14445/23500301/IJAP-V10I2P101

Volume 10 Issue 2, 1-6, May-Aug 2023

Original Article

Transformation of Frequency Dispersion of Electrical Parameters of Liver Tissue Depending on its Storage Temperature

T. V. Pryimak[1], I. M. Gasiuk[2], D. M. Chervinko[3]

[1,2,3]*Vasyl Stefanyk Precarpathian National University, Department of Materials Science and New Technology, Ivano-Frankivsk, Ukraine.*

[2]*Corresponding Author : gasyukim@gmail.com*

Received: 05 April 2023 Revised: 18 May 2023 Accepted: 03 June 2023 Published: 14 June 2023

Abstract *- The article discusses the temporal transformation of the frequency characteristics of electrical parameters of liver tissue during its storage in the temperature range of 2-35 C°. Changes in direct current conductivity, frequency dispersion of the real component of conductivity and tangent of the dielectric loss angle in the frequency range of 0.01 Hz -100 kHz (beta dispersion range) are considered. The relationship between the transformation of thermo-time dependences of electrical parameters and the degree and nature of morphological changes in biological tissue has been established. In particular, it is shown that the local values and the direction of the monotonicity of the polarization relaxation time function in the studied frequency range of electrical impedance spectra measurement can be considered as a criterion for the degree and type of destructive changes in liver tissue when it is stored in an air atmosphere at different temperatures.*

Keywords *- Conductivities, Impedance spectroscopy, Tangents of dielectric loss, Temperatures, Resonant frequencies.*

1. Introduction

Physical research methods of biological tissue are effective ways of establishing a connection between their electrical properties and physical parameters. One of the fast, non-invasive, easy-to-use, and reliable methods of analyzing the structural integrity of biomaterials is the method of complex electrical impedance in a wide frequency range. [1- 8]

Nowadays, EIS is used to estimate the overall impact of low temperatures, thawing and freezing processes, predict the emergence of cancer diseases and functional diagnostics of cancer cells to distinguish them from healthy ones. It could also indicate fluid movement in extensive burns and the cytotoxicity of chemical compounds. [9-15] The assessment of the structural integrity of tissue under conditions of destructive processes and effects can also be performed using EIS. [16,17,27]

For example, in work [16], based on the results of electrical impedance measurement, the authors built equivalent electrical diagrams of liver tissue damaged through the action of destructive factors, including gamma radiation and thiourea. The comparison of the constructed scheme parameters' with the results of the microscopic examination of samples allowed us to establish the presence of potential circuit model elements' correspondence to certain cellular environments and structures. As a result, it is shown that the parameters of equivalent electrical diagrams of tissue impedance, particularly the CPE element, reflect the capacitance of the cell membrane, R1 and R2 - the external and internal resistances, respectively, and R3 - membrane resistance.

In the subsequent work, a detailed analysis of the electric impedance spectrum transformation of tissue exposed to different temperatures over a certain period of time was carried out. [13] Calculation of circuit parameters and observation of the electric circuit structure transformation and their comparison with the results of microscopic analysis allowed us to conclude about the probable dependence of structural and parametric research results on the intensity of the influence of factors. A detailed analysis of decryption parameters helped to build transformational dependencies of samples depending on their level of damage.

The method of creating equivalent circuits, which is actively used in bioimpedance studies, despite its relative ease of use, does not allow to formation a general characteristic of ion transport processes in the tissue environment when using alternating electric current and under conditions of destructive influence.

In the proposed work, an attempt was made to analyze the frequency dispersion of complex electrical parameters of liver tissue under the influence of temperature to determine the peculiarities of charge transfer in its electrolyte subsystem of tissue under different degrees of structural degradation.

2. Materials and Methods

The use of isolated liver tissue for the experiment gave a possibility to control the size of the samples according to the size of the used cells and contributed to more accurate measurement due to the uniform influence of temperature. [19]

Sample cells for research were made from a plastic body of a 2 ml medical syringe—the ends of the cylindrical sample contacted with a nickel mesh. Nickel conductors, welded to the mesh, served as current conductors. The structure of the experimental equivalent scheme was chosen similarly to the one we provided in previous works. [19, 20]

Cylindrical samples, 1.2 cm high, 2 cm in diameter, and weighing 1 – 1.5 g, were placed in a specially designed, hermetic thermostat 1/120 SPU under the influence of temperatures 275K, 281K, 285K, 298K, and 308K for 2, 5, 8, 10, and 14 hours.

Getting of electrical impedance spectra was performed using a standard AUTOLAB PGStat 30 spectrometer in the frequency range of 0.01 Hz – 100 kHz. To reduce the impact of amplitude values of the measurement signal voltage on the condition of organic tissue, the peak potential was reduced to 0 – 5 mV.

The signal recording was performed in automatic mode. Dependencies of real and imaginary values of specific conductivity σ’ and σ’’, dielectric permeabilities ξ’ and ξ’’, and loss angle tangent were built using Origin software. Processing of curves was also carried out using the Origin software.

The frequency dispersion of electrical conductivity and dielectric permeability is determined from the Nyquist diagrams according to equations 4 and 5. Electrical conductivity is determined by equation 1:

$$\Sigma = \frac{1}{Z^*} = \frac{S}{\rho^* \cdot l}, \quad (1)$$

where Z*, ρ* - complex impedance and specific electrical resistance, respectively, and S, l – are the area and thickness of the sample, respectively. where ω = 2πf, ε_0 - electric constant, j =$\sqrt{-1}$.

From the diagram, σ'- (σ" - $\varepsilon_0\varepsilon_\infty\omega$) ($\varepsilon_\infty$ - value of dielectric permeability at high frequencies) in the low-frequency range, the value of specific conductivity at constant current σdc was determined at different temperatures.

The value of ε_∞ is determined from the Cole-Cole diagram ε" - ε' by approximating the experimental curve to the intersection with the abscissa axis. [22]

The real ε' and imaginary ε" dielectric permeabilities are determined by equations 2 and 3:

$$\varepsilon' = \frac{\rho''(\omega)}{(\rho''(\omega))^2+(\rho'(\omega))^2 \cdot \varepsilon 0 \cdot \omega}, \quad (2)$$

$$\varepsilon'' = \frac{\rho'(\omega)}{(\rho''(\omega))^2+(\rho'(\omega))^2 \cdot \varepsilon 0 \cdot \omega}, \quad (3)$$

The frequency dependence of the real component of complex conductivity is determined by equations 4 and 5:

$$\sigma'(\omega)=\frac{\rho'(\omega)}{(\rho''(\omega))^2+(\rho'(\omega))^2} \quad (4)$$

$$\sigma''(\omega)=\frac{\rho''(\omega)}{(\rho''(\omega))^2+(\rho'(\omega))^2} \quad (5)$$

3. Results and Discussion

The Nyquist diagrams experimentally obtained for the studied samples at different temperatures, preserved for 2 - 14 hours, are depicted in Figure 1. The frequency range of the obtained spectra is 0.01 Hz - 100 kHz. Z' and Z" are the real and imaginary components of the impedance, respectively. The insets show the high-frequency regions of the spectra, with arrows indicating the direction of frequency increase.

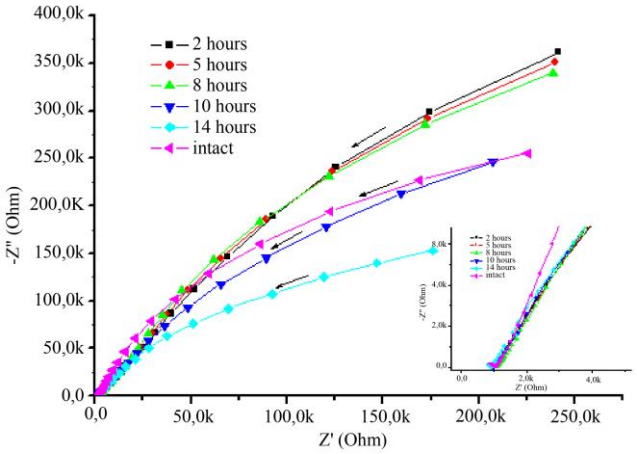

(a)

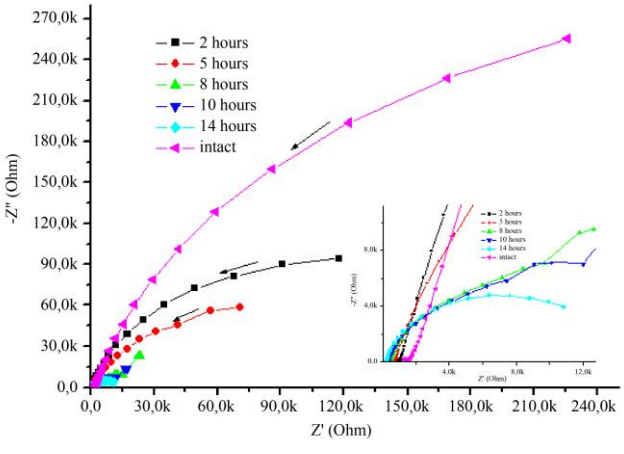

(b)

Fig. 1 Impedance spectra of liver tissue stored at a) 271K, b) 308K

A decrease in the real and imaginary parts of the complex impedance was observed for the entire range of measured frequencies. The general form of the impedance spectrum with a clearly defined polarization loop, the slope

of which decreases with decreasing frequency, corresponds to the model of the equivalent circuit described in the previous work [19]. It includes three R-CPE elements at the initial stages of destruction or two R-CPE elements at the last. This agrees well model of ion charge transfer in a disordered system, which contains an equivalent number of elements corresponding to the number of homogeneity regions.

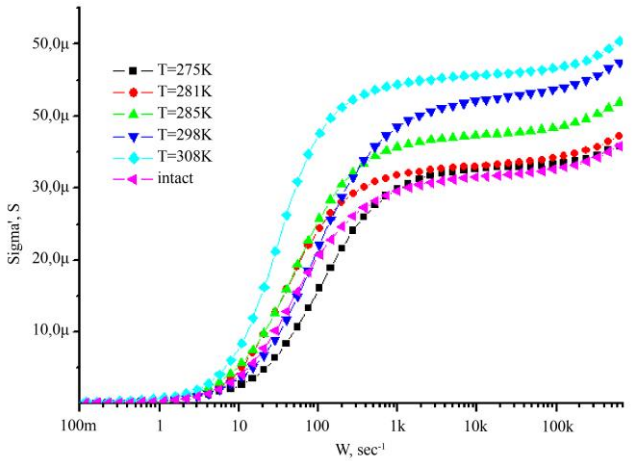

a)

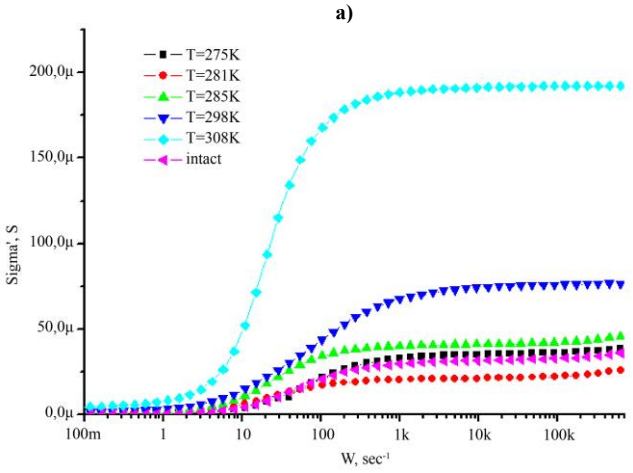

b)

Fig. 2 Spectra of frequency-dependent conductivity of liver samples exposed to a temperature for a) 2 and b) 14 hours

Using the relationship: $R = R' + iR''$, $\sigma = \frac{1}{R} = \frac{1}{R'+iR''} = \frac{R'-iR''}{R'^2+R''^2} = \frac{R'}{R'^2+R''^2} - i\frac{R''}{R'^2+R^{1,2}}$; де $\sigma' = \frac{R'}{R'+R''^2}$ і $\sigma'' = \frac{R''}{R'^2+R''^2}$ – the real and imaginary parts of the system's complex electrical conductivity were calculated, and dependencies of σ'(w) for a selected group of temperatures (Figure 2) was constructed.

A gradual increase in conductivity with the rise of temperature and frequency can be observed (Figure 2a). On the other hand, there is a sharp rise in conductivity at 308K over a 14-hour exposure period, while the level of conductivity is preserved for other temperatures over the same time interval (Figure 2b). The chosen frequency range, between 0.01 Hz – 100 kHz, corresponds to the low-frequency mechanisms of ion polarization depending on their placement relative to the plasma membrane and the passage of current through it, corresponding to the α-dispersion. [23, 24, 25]

This result might be caused by an increased concentration of ions accumulated over a prolonged period of thermal impact in the area of membrane damage.

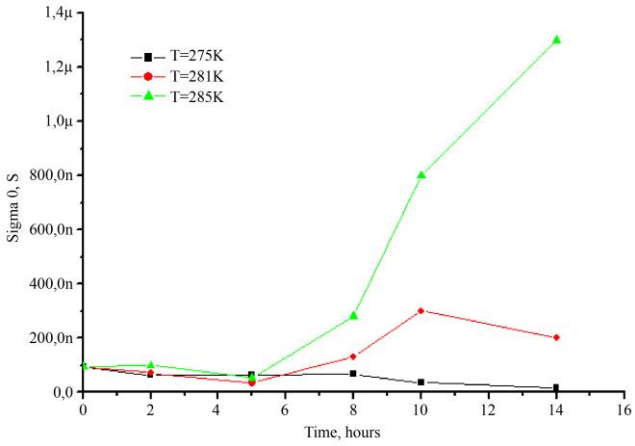

a)

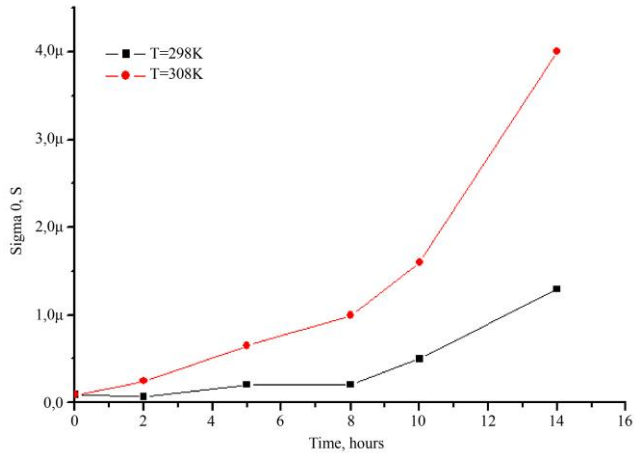

b)

Fig. 3 The spectra of alternating current (AC) conductivity dependence on time

The results of AC conductivity calculations using the Cole-Cole method were used to clarify the behavior of charge carriers in the electrolytic subsystem of the studied samples. [21, 22] The graphs of σ_0 (t) dependence at different temperatures are shown in Figure 3 (a, b).

A tendency towards increased conductivity with increasing temperature and time interval at which the experimental samples were kept was observed (Figure 3a, 3b). As a result of the development of destructive processes, particularly at 308K, an unbalanced state of the studied biological system is formed. The existing concentration gradient at the distribution boundary contributes to systemic polarization, which leads to the emergence of an internal electric field that prevents it from penetrating the external one.

The equalization of the concentration gradient, as a result of the destruction of the plasma membrane, initiated the transition of the system from an anisotropic to an isotropic state, which caused an increase in conductivity as a result of an increase in ion mobility due to the disappearance of the distribution boundary, which we confirmed in morphological studies in previous work. [19]

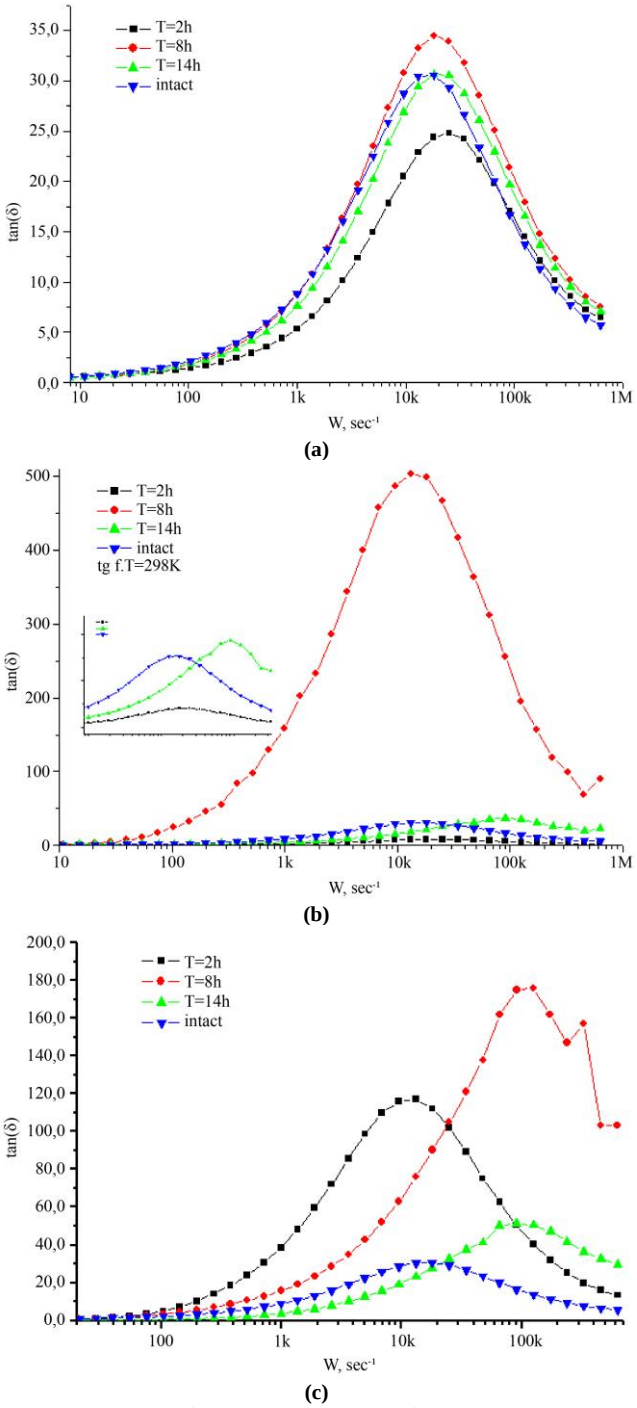

Fig. 4 Dependence of the loss tangent on the frequency at a) 275K, b) 298K, and c) 308K. The inset shows the high-frequency region of the spectrum

The dielectric loss angle tangent values were calculated to better understand the peculiarities of dipole reorientation processes under the influence of an external variable sinusoidal electric field. The graphs of the dependence of tg δ (ω) are presented in Figure 4.

The character of the dependence of the loss angle tangent on frequency is extreme. The increase in the minimum value of the loss angle tangent over time is due to the formation of a large number of dipoles of a certain size in connection with extensive destruction (Figure 4a, 4b). Histological analysis of samples under the influence of such temperatures demonstrates the formation of local tissue damage, blurring of the contours of liver sample hepatocytes, and an increase in intercellular spaces. This picture may indicate damage to the plasma membrane and, as a result, a decrease in resistance and an increase in permeability, which is reflected in the change in the structure of the equivalent circuit from six- to five- and four-element, in particular, at 308K. [19]

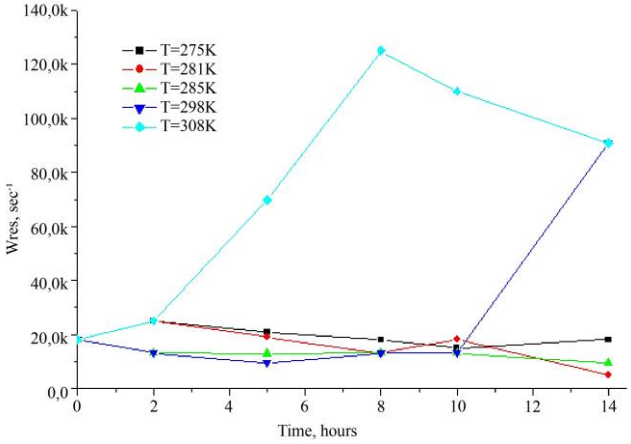

Fig. 5 Spectra of the resonance frequency dependence on time at various temperatures: a) 275K, b) 281K, c) 285K, d) 298K, and e) 308K

Based on the calculations of tgδ (ω), the position of the peaks on the curve was used to determine the dependence ω_{res} (t). The graphs of dependence are presented in Figure 6.

There is a clear trend of the resonance frequency decreasing with a reduction in temperature and frequency, corresponding to forming a larger dipole.

An increase in temperature, in addition to damaging the membrane, is reflected through an increase in the tangent of the loss angle and the resonance frequency, which is caused by an increase in the number of small-sized dipoles, which could be fragments of membrane components and elements of intracellular organelles. This corresponds to the reduced values of the CPE- and R- parameters of the samples under the influence of 298K and 308K, compared to intact ones. [19]

In addition, at high temperatures, due to membrane destruction, a large number of sources of dipole polarization appear, which also contributes to an increase in ω_{res}.

Therefore, as a whole, the processes of tissue destruction, under the influence of temperature, are reflected in the decrease in complex resistance, both real and imaginary, which can be associated with the structural

destruction of the membrane, which also contributes to its increased permeability (Figure 1a, 1b).

In particular, an increase in the concentration of charge carriers, both external and intracellular, in the areas of destruction contributes to an increase in conductivity (Figure 2a, 2b) on AC and the disappearance of the distribution boundary. This process causes greater mobility of the accumulated amount of ions, leading to increased conductivity on DC (Figure 3a, 3b).

Elements of a destroyed membrane and a high concentration of ions cause the formation of a large number of dipoles (Figure 4a, 4b) of a relatively small size, which is observed when applying an external, variable electric field (Figure 5).

4. Conclusion

The study of the parameters of the Nyquist diagrams of liver tissue stored in a certain time range at different temperatures confirms the two-stage destruction process. According to it, there is a change in the concentration and composition of charge carriers at the first stage without vivid signs of the destruction of the morphological structure. The second stage implies structural changes and, obviously, leads to irreversible destruction. Storing liver tissue at low temperatures (275K – 285K) leads to minor changes in the ionic subsystem, while an increase in temperature and storage duration leads to drastic changes in the tissue, which, in turn, is reflected by the kinetics of the impedance spectrum parameters. The main indicators of the destruction degree nature can serve as a resonance frequency determined from the frequency dependence of the tangent of dielectric losses.

At the initial stages of destruction, the time dependence of ω_{res} has a descending character. A time increase in this value accompanies the second stage of destructive changes. Such a characteristic may, in the future, become a technologically controllable quantity for creating a method of the fast and non-invasive characteristic of overall damage, potential changes in ionic composition, and degree of destruction of both cells and organs as a whole.

Funding statement

This work is supported by Vasyl Stefanyk Precarpathian National University and the Department of Materials Science and New Technology.

References

[1] Michal M. Radai, Shimon Abboud, and Boris Rubinsky, “Evaluation of the Impedance Technique for Cryosurgery in a Theoretical Model of the Head,” *Cryobiology*, vol. 38, no. 1, pp. 51-59, 1999. [CrossRef] [Google Scholar] [Publisher Link]

[2] K Sunshine Osterman et al. “Non-Invasive Assessment of Radiation Injury with Electrical Impedance Spectroscopy,” *Physics in Medicine and Biology*, vol. 49, no. 5, pp. 665-683, 2004. [CrossRef] [Google Scholar] [Publisher Link]

[3] Marcin Frączek et al., “Measurements of Electrical Impedance of Biomedical Objects,” *Acta of Bioengineering and Biomechanics*, vol. 18, no. 1, pp. 11-17, 2016. [CrossRef] [Google Scholar]

[4] Xinru Fan et al. “Estimating Freshness of Ice Storage Rainbow Trout Using Bioelectrical Impedance Analysis,” *Food Science & Nutrition*, vol. 9, no. 1, pp. 154-163, 2020. [CrossRef] [Google Scholar] [Publisher Link]

[5] Yu Wu et al., "Electrical Impedance Tomography for Biomedical Applications: Circuits and Systems Review," *IEEE Open Journal of Circuits and Systems*, vol. 2, pp. 380-397, 2021. [CrossRef] [Google Scholar] [Publisher Link]

[6] A. Kobayashi et al., “Changes of Electrical Impedance Characteristic of Pork in Heating Process,” *International Proceedings of Chemical, Biological & Environmental Engineering*, vol. 50, no. 7, pp. 74-78., 2013. [Google Scholar] [Publisher Link]

[7] Franciny C Schmidt et al., “Assessing Heat Treatment of Chicken Breast Cuts by Impedance Spectroscopy,” *Food Science and Technology International*, vol. 23, no. 2, pp. 110-118, 2017. [CrossRef] [Google Scholar] [Publisher Link]

[8] Matthäus Ernstbrunner et al., “Bioimpedance Spectroscopy for Assessment of Volume Status in Patients Before and After General Anaesthesia,” *PloS one*, vol. 10, no. 3, 2015. [CrossRef] [Google Scholar] [Publisher Link]

[9] G Fischer et al., “Impedance and Conductivity of Bovine Myocardium during Freezing and Thawing at Slow Rates - Implications for Cardiac Cryo-Ablation,” *Medical Engineering & Physics*, vol. 74, pp. 89-98, 2019. [CrossRef] [Google Scholar] [Publisher Link]

[10] Tian-Hua Yu, Jing Liu, and Yi-Xin Zhou, “Using Electrical Impedance Detection to Evaluate the Viability of Biomaterials Subject to Freezing or Thermal Injury,” *Analytical and Bioanalytical Chemistry*, vol. 378, no. 7, pp. 1793-800, 2004. [CrossRef] [Google Scholar] [Publisher Link]

[11] Ethan K Murphy et al. “Comparative Study of Separation Between Ex Vivo Prostatic Malignant and Benign Tissue using Electrical Impedance Spectroscopy and Electrical Impedance Tomography,” *Physiological Measurement*, vol. 38, no. 6, pp. 1242-1261, 2017. [CrossRef] [Google Scholar] [Publisher Link]

[12] Shlomi Laufer et al., “Electrical Impedance Characterization of Normal and Cancerous Human Hepatic Tissue,” *Physiological Measurement*, vol. 31, no. 7, pp. 995-1009, 2010. [CrossRef] [Google Scholar] [Publisher Link]

[13] Pippa Kenworthy et al., “An Objective Measure for the Assessment and Management of Fluid Shifts in Acute Major Burns,” *Burns & Trauma*, vol. 6, no 3, 2018. [CrossRef] [Google Scholar] [Publisher Link]

[14] Laura Ceriotti et al., “Assessment of Cytotoxicity by Impedance Spectroscopy,” *Biosensors & Bioelectronics*, vol. 22, no. 12, pp. 3057-63, 2007. [CrossRef] [Google Scholar] [Publisher Link]

[15] V Lopresto et al., “Temperature Dependence of Thermal Properties of Ex Vivo Liver Tissue Up to Ablative Temperatures,” *Physics in Medicine and Biology*, vol. 64, no. 10, 2019. [CrossRef] [Google Scholar] [Publisher Link]

[16] Andrew A. Gage et al., "Tissue Impedance and Temperature Measurements in Relation to Necrosis in Experimental Cryosurgery," *Cryobiology*, vol. 22, no. 3, pp. 282-288, 1985. [CrossRef] [Google Scholar] [Publisher Link]

[17] Angela A Pathiraja et al., "The Clinical Application of Electrical Impedance Technology in the Detection of Malignant Neoplasms: A Systematic Review," *Journal of Translational Medicine*, vol. 18, no. 227, 2020. [CrossRef] [Google Scholar] [Publisher Link]

[18] A. Aasha, S. Abirami, and M. Anitha, "Effective Optical Communication using Design of Delay Line Filter," *SSRG International Journal of Electronics and Communication Engineering*, vol. 5, no. 1, pp. 16-18, 2018. [CrossRef] [Google Scholar] [Publisher Link]

[19] Taras Pryimak et al., "Electrical Impedance Spectrum Transformation of Liver Tissue under the Influence of Temperature," *International Journal of Engineering Research and Applications*, vol. 11, no. 12, pp. 1–11, 2021. [Google Scholar] [Publisher Link]

[20] T. V. Pryimak et al., "Transformation of the Electrical Impedance Spectra of Biological Tissueunder the Influence of Destructive Factors," *Materials Today: Proceedings*, vol. 62, no. 9, pp. 5796-5799, 2022. [CrossRef] [Publisher Link]

[21] Andrey Tarasov, and Konstantin Titov, "On the use of the Cole–Cole Equations in Spectral Induced Polarization," *Geophysical Journal International*, vol. 195, no. 1, pp. 352–356, 2013. [CrossRef] [Google Scholar] [Publisher Link]

[22] N. M. Olekhnovich, Yu. V. Radyush, and A. V. Pushkarev, "Mechanisms of dielectric polarization in perovskite ceramics of the relaxor ferroelectrics (1 − x)(NaBi)1/2TiO3−x Bi(ZnTi)1/2O3 (x < 0.2)," *Physics of the Solid State*, vol. 54, 2236 – 2242, 2012. [CrossRef] [Publisher Link]

[23] Sara Abasi et al., "Bioelectrical Impedance Spectroscopy for Monitoring Mammalian Cells and Tissues under Different Frequency Domains: A Review," *ACS Measurement Science Au*, vol. 2, no.6, pp. 495-516, 2022. [CrossRef] [Google Scholar] [Publisher Link]

[24] D A Dean et al., "Electrical Impedance Spectroscopy Study of Biological Tissues," *Journal of electrostatics*, vol. 66, no. 3-4, pp. 165-177, 2008. [CrossRef] [Google Scholar] [Publisher Link]

[25] Damijan Miklavčič, Nataša Pavšelj, and Francis X. Hart, "Electric Properties of Tissues," *Encyclopedia of Biomedical Engineering*, *Wiley-Interscience*, Hoboken, pp. 1-12, 2006. [CrossRef] [Google Scholar] [Publisher Link]

[26] Haylemaryam Gashaw Geto et al., "Design and Analysis of Rectangular Micro-strip Patch Antenna for Handheld Cell Phones," *SSRG International Journal of Electronics and Communication Engineering*, vol. 6, no. 7, pp. 11-14, 2019. [CrossRef] [Publisher Link]

[27] Susana Fuentes-Vélez et al., "Electrical Impedance-Based Characterization of Hepatic Tissue with Early-Stage Fibrosis," *Biosensors*, vol. 12, no. 2, p. 116, 2022. [CrossRef] [Google Scholar] [Publisher Link]